

Vacuum infiltration of copper aluminate by liquid aluminium

M. Guedes^{1,}, J. M. F. Ferreira², L. A. Rocha³, A. C. Ferro⁴*

¹Department of Mechanical Engineering, Escola Superior de Tecnologia, Instituto Politécnico de Setúbal,
2910-761 Setúbal, Portugal/ICEMS.

²Department of Ceramics and Glass Engineering/CICECO, Universidade de Aveiro, 3810-193 Aveiro,
Portugal.

³Department of Mechanical Engineering/CT2M, Universidade do Minho, Campus de Azurém, 4800-058,
Guimarães, Portugal.

⁴Department of Chemical and Biological Engineering/ICEMS, Instituto Superior Técnico, UTL, Av.
Rovisco Pais, 1049-001 Lisboa, Portugal.

*Corresponding author. Tel.: +351 265790000; fax: +351 265721869; e-mail:

mafalda.guedes@estsetubal.ips.pt

Abstract

This paper studies attained microstructures and reactive mechanisms involved in vacuum infiltration of copper aluminate preforms with liquid aluminium. At high temperatures, under vacuum, the inherent alumina film enveloping the metal is overcome, and aluminium is expected to reduce copper aluminate, rendering alumina and copper. Under this approach, copper aluminate toils as a controlled infiltration path for aluminium, resulting in reactive wetting and infiltration of the preforms.

Ceramic preforms containing a mixture of Al_2O_3 and CuAl_2O_4 were infiltrated with aluminium under distinct vacuum levels and temperatures, and the resulting reaction and infiltration behaviour is discussed. Copper aluminates stability ranges depend on oxygen partial pressure; selection of infiltration temperature and vacuum level determines both CuAl_2O_4 and CuAlO_2 ability for liquid aluminium infiltration. At 1100°C and $p\text{O}_2 = 0.16$ atm, reactive infiltration is achieved *via* reaction between

1 aluminium and CuAl_2O_4 ; however, fast formation of an alumina layer blocking liquid aluminium wicking
2 results in incipient infiltration. At $1000\text{ }^\circ\text{C}$ and $p\text{O}_2 = 8 \times 10^{-8}$ atm, CuAlO_2 decomposes to Cu and Al_2O_3
3 and infiltration of the ceramic is hindered by the non-wetting behaviour of the resulting metal alloy. At
4 $1000\text{ }^\circ\text{C}$ and $p\text{O}_2 = 4 \times 10^{-7}$ atm, extensive infiltration is achieved *via* redox reaction between aluminium
5 and CuAlO_2 , rendering a microstructure characterised by uniform distribution of alumina particles amid
6 an aluminium matrix.
7

8
9 This work evidences that liquid aluminium infiltration upon copper aluminate-rich preforms is a
10 feasible route to produce Al-matrix alumina-reinforced composites. The associated reduction reaction
11 renders alumina, as fine particulate composite reinforcements, and copper, which dissolves in liquid
12 aluminium contributing as a matrix strengthener.
13

14
15
16
17
18
19
20
21
22
23 **Keywords:** Reactive Aluminium Infiltration; B. Composites; B. Microstructure-final; D. Spinels.
24

25 26 27 1. Introduction

28
29 Chemical reactions between liquid aluminium and ceramics are being increasingly studied has a route for
30 synthesising metal/ceramic composites. The reaction front between aluminium and the ceramic surfaces
31 migrates throughout the solid, leaving behind a mixture of solid ceramic reaction products and metallic
32 liquid [1-3]. Reaction thus induces wetting and promotes infiltration.
33

34
35 However, the inherent formation of a stable alumina film enveloping the metal (reaction 1) is a major
36 issue in aluminium reactive infiltration, because it prevents a true metal/ceramic interface to form and
37 wetting and infiltration to occur.
38



40
41
42
43
44
45
46
47
48
49
50
51 At room temperature the alumina film thickness varies from around 10 nm (STP conditions) to 2 nm
52 (after deep pickling) [4]. Alumina film breakup has been found at temperatures around $1000\text{ }^\circ\text{C}$ under
53 high vacuum conditions [4-9], in a process controlled by film reduction in the presence of aluminium
54 liquid (reaction 2) [3,4,9].
55
56
57
58
59
60
61
62
63
64
65



Progression of reaction (2) lessens the alumina layer, promoting its destabilisation. Al_2O_3 reduction occurs if oxygen availability at the surface of the film is lower than the produced oxygen flow, which is proportional to Al_2O partial pressure [10]. Al_2O partial pressure was reported between 10^{-10} atm at 860 °C [4] and 3×10^{-6} atm at 1100 °C [11]. High vacuum is thus a reliable process to effectively destabilize the alumina film enveloping aluminium.

The Al-Cu-O is an interesting system for development of Al-matrix composites through aluminium reactive infiltration involving the system's copper oxides (CuO , Cu_2O) or copper aluminates (CuAl_2O_4 , CuAlO_2). Some studies have been published concerning reaction between liquid aluminium and copper oxide [12-17]. Copper oxide reduction by aluminium renders reinforcement alumina particles and copper, which enters the metal matrix as alloying element. However, the process cannot be carried out under high vacuum, since copper oxides dissociation under low oxygen partial pressure occurs at low temperatures [18,19]. Under atmospheric pressure attained reaction and infiltration are typically small.

Copper aluminates, CuAl_2O_4 and CuAlO_2 , are on their turn less sensitive to oxygen pressure than copper oxides, presenting a broader stability range under vacuum. For example, according to Rogers *et al.* [20], at 1000 °C CuAlO_2 dissociation to alumina, copper and oxygen (reaction 3) takes place at $p_{\text{O}_2} = 6.0 \times 10^{-7}$ atm, and CuAl_2O_4 dissociation to CuAlO_2 , alumina and oxygen (reaction 4) takes place at $p_{\text{O}_2} = 4.4 \times 10^{-2}$ atm. According to Gibbs free energy calculations by Jacob & Alcock [21], at 1100°C reaction (4) takes place at oxygen partial pressure below 0.11 atm.



In as much, approaching reactive infiltration in the Al-Cu-O system by using copper aluminate as the liquid infiltration path allows the use of high vacuum conditions.

2. Materials and methods

2.1. Preparation of CuAl_2O_4 -rich preforms

CuAl_2O_4 was produced from solid state reaction between Al_2O_3 (CT-1200-SG, ALMATIS; max. 0.34 wt% impurities; $d_{50} = 1.12 \pm 0.02 \mu\text{m}$) and CuO (MERCK; max. 0.4 wt% impurities; $d_{50} = 1.85 \pm 0.01 \mu\text{m}$). A 55 mol%- Al_2O_3 /45 mol%- CuO mixture was homogenized, heated in air at $5^\circ\text{C}/\text{min}$ up to 1100°C with 15 min holding, and cooled inside the furnace. XRD (PW 3020, PHILIPS) showed that CuO is completely eliminated under those conditions, and that CuAl_2O_4 and residual Al_2O_3 are the only crystalline phases identified within the equipment's detection limit (Fig. 1). The resulting material was comminuted by planetary ball milling (PM100, RETSCH). Attained powders ($d_{50} = 1.29 \pm 0.13 \mu\text{m}$) were mixed with 1.5 wt% binder (Duramax B1000, RHOM & HAAS) and used to produce discs (approx. 2 g, \varnothing 13 mm) by uniaxial dry pressing. Discs were heated up to 300°C at $5^\circ\text{C}/\text{min}$, with 30 minutes holding for debinding.

2.2. Infiltration

Ceramic discs were fitted inside a hollow aluminium part (MOZAL, 99.85%), placed in an alumina crucible, and heated up at $5^\circ\text{C}/\text{min}$ followed by 1 h holding (prototype vertical vacuum furnace). A 3 kPa gravity load was applied to enhance Al/ceramic contact. Aluminium parts were thoroughly cleaned by sonication in NaOH 1M solution at 80°C for 10 minutes, rinsed with distilled water and dried, immediately before infiltration.

Samples cooled inside the furnace, and the resulting microstructures were investigated by FEG-SEM (JSM-7001F, JEOL) and EDS (Inca pentaFETx3, OXFORD INSTRUMENTS).

3. Results and discussion

As previously discussed, copper oxidation state (0, +1 or +2) depends on temperature and oxygen partial pressure, conditioning copper aluminate stability.

Under $p\text{O}_2 = 0.16 \text{ atm}$ and 1100°C , CuAl_2O_4 is the copper aluminate present in the preform. Fig. 2 renders general microstructural features of a sample infiltrated under these conditions. Reaction front does not progress significantly into the ceramic preform, and liquid aluminium infiltration is irregular and limited. The maximum observed penetration depth is in the order of $350 \mu\text{m}$.

Two regions can be assigned next to the aluminium source: an intermediate dense infiltrated region, and unreacted, partially densified, ceramic preform. The infiltrated region (Fig. 3) is composed by an alumina irregular layer, surrounded in all its extension by a mixture of two phases. EDS analysis assigned the presence of Cu and O to one of the phases, thus identified as copper oxide. The attained Cu:Al ratio \approx 1 in the other phase suggests the presence of CuAlO₂. Small formations of the same phases are also distributed throughout the alumina layer.

These results suggest a reactive infiltration mechanism were liquid aluminium leaving the metal source reacts with CuAl₂O₄ through the CuO groups in the spinel phase, according to reaction (5):



This reaction leads to rapid formation of fresh alumina between the starting alumina particles, with copper being release into the liquid. When the alumina layer becomes continuous, infiltration stops, hindering Al access to the ceramic preform. The Cu-containing aluminium liquid between the alumina formations and the ceramic preform quickly wears out of Al through reaction (5). Remaining copper liquid entrapped near alumina reacts to form CuAlO₂ according to reaction (6). Oxygen permeating through the pore structure plays an important role in this reaction [14,22].



In as much, under $p_{\text{O}_2} = 0.16$ atm and 1100°C, incipient infiltration is achieved *via* reaction between aluminium and CuAl₂O₄; nevertheless fast formation of an alumina layer blocks liquid aluminium wicking, hindering infiltration.

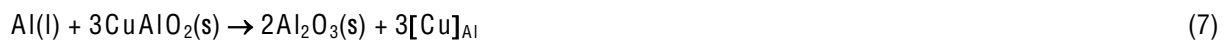
Under $p_{\text{O}_2} \approx 8 \times 10^{-8}$ atm and 1000 °C, CuAlO₂ is the copper aluminate present in the starting preform. Metal/powder mingling appears to have occurred in few locations at the metal/ceramic borders (Fig. 4), which attests that the alumina layer enveloping liquid aluminium is destabilized. But under these conditions, infiltration does not take place. Instead, the aluminate decomposition (reaction 3) is triggered [20], and copper dissolves into aluminium liquid. As follows, neither reactive infiltration nor spontaneous infiltration are possible, respectively because the reactive infiltration mechanism is no longer available,

1 and because the contact angle between the resulting Al-Cu alloy and the ceramic is not sufficiently low to
2 drive capillary rise.
3

4 Under $pO_2 = 4 \times 10^{-7}$ atm and 1000 °C, $CuAlO_2$ is the copper aluminate present in the starting preform
5 [20]. Fig. 5 renders a general view of the sample, showing extensive infiltration and reaction. The
6 corresponding microstructure presents three distinct regions: the aluminium source; a dense infiltrated
7 region approximately 900 μm thick; and unreacted, partially densified, ceramic preform in the sample
8 centre.
9

10 The metal layer is composed by primary (Al) phase and (Al)/ θ eutectic, distributed throughout. Fig. 6
11 shows a general view of the metal/infiltration layer interface. Unreacted starting alumina particles are
12 visible, merged in a background containing three phases (Fig. 7). EDS analysis assigned the presence of
13 aluminium and oxygen to the abundant round-shaped particles, thus identified as alumina. The
14 intergranular phase was assigned to aluminium. The light regions contain copper and aluminium in a 0.53
15 atomic ratio, and were assigned to solidified Al-Cu alloy (θ phase).
16

17 These results suggest a reactive mechanism where liquid aluminium leaving the metal source reacts
18 with $CuAlO_2$ through the Cu_2O groups in the aluminate phase, according to reaction (7).
19
20



22 As a result, fresh alumina forms between the starting alumina particles, and copper is released into the
23 liquid. The process is similar to reaction (5), but with lower alumina delivery. Apparently, the alumina
24 formation kinetics is now sufficiently slow to allow extensive infiltration of liquid aluminium, and
25 considerable amounts of copper reach the metal source, rendering θ phase on cooling. Formed Al_2O_3
26 particles are approximately round (Fig. 8) and mostly of the micron order (much smaller than the size of
27 the starting alumina particles). Apparently all $CuAlO_2$ in the reaction layer was consumed in the course of
28 reaction (7), toiling as a controlled infiltration path for liquid Al.
29

30 It can be concluded that liquid aluminium infiltration of $Al_2O_3/CuAlO_2$ green bodies is possible at
31 1000°C under $pO_2 = 4 \times 10^{-7}$ atm. Under these conditions $CuAlO_2$ does not decompose. The use of high
32 vacuum promotes destabilisation of the inherent alumina film enveloping liquid aluminium, creating
33 conditions for enhanced contact between aluminium and the ceramic. Reactive infiltration is achieved *via*
34
35
36
37
38
39
40
41
42
43
44
45
46
47
48
49
50
51
52
53
54
55
56
57
58
59
60
61
62
63
64
65

1 redox reaction between aluminium and CuAlO_2 , rendering a microstructure characterised by alumina
2 particles distributed amid an aluminium matrix.
3
4
5
6

7 4. Conclusions

8
9 Ceramic preforms containing Al_2O_3 and CuAl_2O_4 were infiltrated with liquid aluminium under
10 vacuum and the resulting wetting and infiltration mechanisms were studied. Depending on the infiltration
11 temperature and oxygen partial pressure, the stable copper aluminate in the preform is either CuAl_2O_4 or
12 CuAlO_2 .
13
14
15

16 Under $p_{\text{O}_2} = 0.16$ atm and 1100 °C, infiltration is achieved *via* reaction between aluminium and
17 CuAl_2O_4 in the preform. Nevertheless, fast formation of an alumina layer blocks liquid aluminium
18 wicking and results in irregular and hindered infiltration.
19
20
21

22 Under $p_{\text{O}_2} = 8 \times 10^{-8}$ atm and 1100 °C, CuAlO_2 is the copper aluminate present in the starting preform.
23 CuAlO_2 decomposes to Cu and Al_2O_3 , and infiltration is hindered because no reactive infiltration
24 mechanism is available.
25
26
27

28 Under $p_{\text{O}_2} = 4 \times 10^{-7}$ atm and 1000 °C, CuAlO_2 is the aluminate present in the starting preform. Under
29 these conditions CuAlO_2 does not decompose. Extensive metal infiltration is achieved *via* reaction
30 between liquid aluminium and Cu_2O groups in the copper aluminate. Attained microstructure is
31 characterized by uniform distribution of Al_2O_3 particles amid an aluminium matrix.
32
33
34
35
36

37 This work demonstrates that liquid aluminium infiltration of copper aluminate green bodies is a
38 practicable route to produce Al-matrix alumina-reinforced composites. The preliminary results reported
39 show that at 1000 °C extensive infiltration takes place under a vacuum level that destabilises the alumina
40 enveloping film while avoiding decomposition of the aluminates. Reactive infiltration is promoted by the
41 redox reaction between Al and copper aluminate, with full consumption of the latter. The reaction renders
42 alumina precipitates and metallic copper (which dissolves in liquid alumina) as reaction products, thus
43 combining *in situ* particle reinforcement with *in situ* alloying.
44
45
46
47
48
49
50
51

52 Acknowledgements

53
54
55
56
57
58
59
60
61
62
63
64
65

1 The authors are grateful to Teresa Marcelo (LNEG) for helpful discussions and use of lab facilities, and to
2
3 Paulo Machado (EST/IPS) for assistance in experimental issues. MG acknowledges FCT for financial
4
5 support under contract SFRH/BD/25711/2005.
6
7

8 9 References

- 10 [1] Hillig, W. B., Mcguigan, H. C., An exploratory study of producing non-silicate all-oxide composites
11 by melt infiltration, *Mater. Sci. Eng. A* 196 (1995) 183-190.
12
13 [2] Kumar, P., Travitzky, N. A., Beyer, P., Sandhage, K. H., Janssen, R., Claussen, N., Reactive casting
14 of ceramic composites (r-3c), *Scr. Mater.* 44 (2001) 751-757.
15
16 [3] Naga, S. M., El-Maghraby, A., El-Rafei, A. M., Properties of ceramic-metal composites formed by
17 reactive metal penetration, *Am. Ceram. Soc. Bull.* 86 (2007) 9301-U9319.
18
19 [4] Eustathopoulos, N., Joud, J. C., Desre, P., Hicter, J. M., The wetting of carbon by aluminium and
20 aluminium alloys, *J. Mater. Sci.* 9 (1974) 1233-1242.
21
22 [5] Klintner, A. J., Leon-Patiño, C. A., Drew, R. A. L., Wetting phenomena of Al-Cu alloys on sapphire
23 below 800°C, *Acta Mater.* 58 (2010) 1350-1360.
24
25 [6] Landry, K., Kalogeropoulou, S., Eustathopoulos, N., Wettability of carbon by aluminum and
26 aluminum alloys, *Mater. Sci. Eng. A* 254 (1998) 99-111.
27
28 [7] Laurent, V., Chatain, V., Eustathopoulos, N., Wettability of SiC by aluminum and Al-Si alloys, *J.*
29 *Mater. Sci.* 22 (1987) 244-250.
30
31 [8] Saiz, E., Tomsia, A. P., Sukanuma, K., Wetting and strenght issues at Al/ α -alumina interfaces, *J. Eur.*
32 *Ceram. Soc.* 23 (2003) 2787-2796.
33
34 [9] Ferro, A. C., Derby, B., Wetting behaviour in the al-si/sic system: Interface reactions and solubility
35 effects, *Acta Metall. Mater.* 43 (1995) 3061-3073.
36
37 [10] Landry, K., Kalogeropoulou, S., Eustathopoulos, N., Naidich, Y., Krasovsky, V., Characteristic
38 contact angles in the aluminium/vitreous carbon system, *Scr. Mater.* 34 (1996) 841-846.
39
40 [11] Coudurier, L., Adorian, J., Pique, D, Eustathopoulos, N., Study of wettability by liquid aluminum of
41 alumina and alumina covered with a layer of a metal or a refractory compound, *Rev. Int. Hautes Tempér.*
42 *Refract.* 21 (1984) 81-93.
43
44
45
46
47
48
49
50
51
52
53
54
55
56
57
58
59
60
61
62
63
64
65

- 1 [12] Guedes, M., Ferreira, J. M. F, Ferro, A. C., Reaction mechanisms in Al_2O_3 -CuO preforms infiltration
2 by liquid aluminium, (submitted)
3
4 [13] Huang, Z. J., Yang, B., Cui, H., Duan, X. J., Zhang, J. S. , Microstructure of designed al matrix
5 composites reinforced by combining *in situ* alloying elements and $\text{Al}_2\text{O}_3(\text{p})$, J. Mater. Sci. Lett. 20 (2001)
6 1749 - 1751.
7
8 [14] Huang, J.-Z., Yang, B., Cui, H., Zhang, J. S., Study on the fabrication of Al matrix composites
9 strengthened by combined in-situ alumina particle and in-situ alloying elements, Mater. Sci. Eng. A 351
10 (2003) 15-22.
11
12 [15] Chen, G., Sun, G.-X., Zhu, Z.-G., Study on reaction-processed Al-Cu/ α - $\text{Al}_2\text{O}_3(\text{p})$ composites, Mater.
13 Sci. Eng. A 265 (1999) 197-201.
14
15 [16] Chen, G., Sun, G.-X., Zhu, Z., On the chemical reactions to process particle reinforced Al-Cu alloy
16 matrix composites, Mat. Sci. Eng. A 251 (1998) 226-231.
17
18 [17] Kobashi, M., Choh, T., Fabrication of particulate composite by in situ oxidation process, Light
19 Metals 42 (1992) 138-142
20
21 [18] Johnson, R. E., Rhines, F. N., Cu-o, in: T. Lyman (Ed.), Metals Handbook, vol. 8 - Metallography,
22 structures and phase diagrams, 8th ed, ASM International, Ohio, 1973, pp. 298-357.
23
24 [19] Hallstedt, B., Risold, D., Gauckler, L. J., Thermodynamic assessment of the copper-oxygen system,
25 J. Phase Equilib. 15 (1994) 483-498.
26
27 [20] Rogers, K. A., Trumble, K. P., Dalgleish, B. J., Reimanis, I. E., Role of oxygen in microstructure
28 development at solid-state diffusion-bonded Cu/ α - Al_2O_3 interfaces, J. Am. Ceram. Soc. 77 (1994)
29 2036-2042.
30
31 [21] Jacob, K. T., Alcock, C. B., Thermodynamics of CuAlO_2 and CuAl_2O_4 and phase-equilibria in
32 system Cu_2O - CuO - Al_2O_3 , J. Am. Chem. Soc. 58 (1975) 192-195.
33
34 [22] Rao, B. S., Jayaram, V., Pressureless infiltration of Al-Mg based alloys into Al_2O_3 preforms:
35 Mechanisms and phenomenology, Acta Mater. 49 (2001) 2373-2385.
36
37
38
39
40
41
42
43
44
45
46
47
48
49
50
51
52
53

54 Figure Captions
55
56
57
58
59
60
61
62
63
64
65

1 Figure 1. XRD results concerning Al₂O₃/CuO mixture (a) green; (b) after 15 min holding time at 1100°C
2
3 (in air) and slow cooling. ■ alumina; ○ CuAl₂O₄, △ CuO.
4
5

6
7 Figure 2. Low magnification secondary electron image (SEI) of sample infiltrated at 1100 °C under pO₂
8 = 0.16 atm.
9

10
11
12 Figure 3. Backscattered electron image (BEI) of sample infiltrated at 1100 °C under pO₂ = 0.16 atm:
13 detail of the interface between infiltration layer and starting preform.
14
15

16
17
18 Figure 4. Low magnification SEI of sample infiltrated under pO₂ = 8x10⁻⁸ atm at 1000 °C (rectangle:
19 incipient metal/ceramic reaction).
20
21

22
23
24
25 Figure 5. Low magnification BEI of infiltrated sample (1000 °C, pO₂ = 4x10⁻⁷ atm).
26
27

28
29 Figure 6. SEI of infiltrated sample (1000 °C, pO₂ = 4x10⁻⁷ atm): transition between metal source and
30 infiltration layer.
31
32

33
34
35 Figure 7. BEI of infiltrated sample (1000 °C, pO₂ = 4x10⁻⁷ atm): detail of the infiltration layer.
36
37

38
39 Figure 8. BEI of infiltrated sample (1000 °C, pO₂ = 4x10⁻⁷ atm): detail of formed alumina particles
40 dispersed in Al matrix.
41
42
43
44
45
46
47
48
49
50
51
52
53
54
55
56
57
58
59
60
61
62
63
64
65

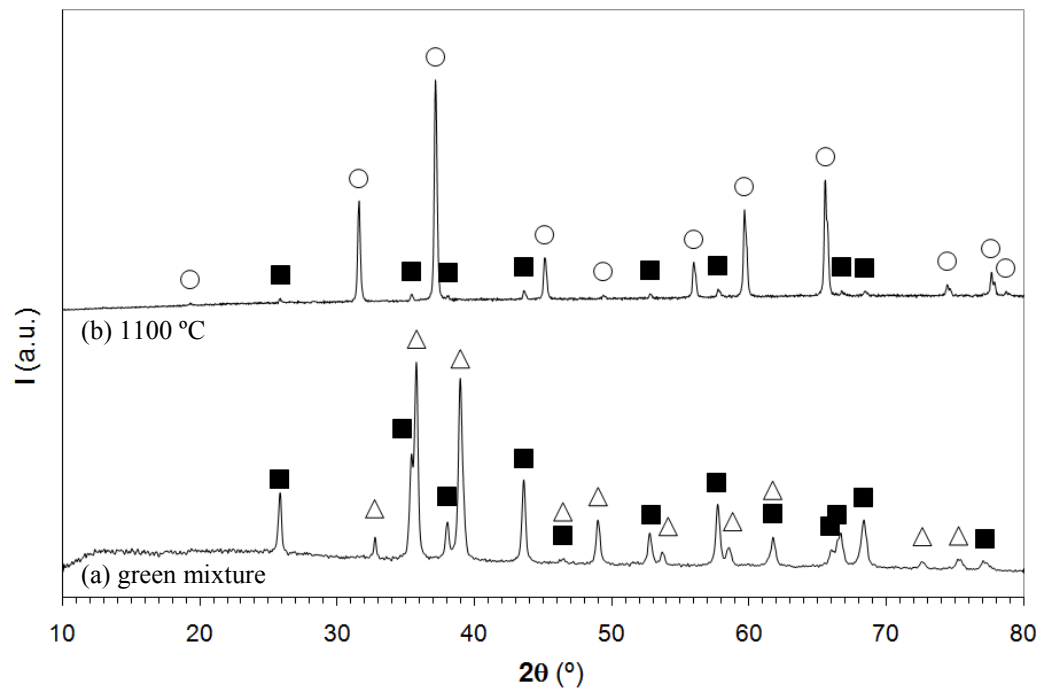


Figure 1. XRD results concerning $\text{Al}_2\text{O}_3/\text{CuO}$ mixture (a) green; (b) after 15 min holding time at 1100°C (in air) and slow cooling. ■ alumina; ○ CuAl_2O_4 , Δ CuO.

Figure

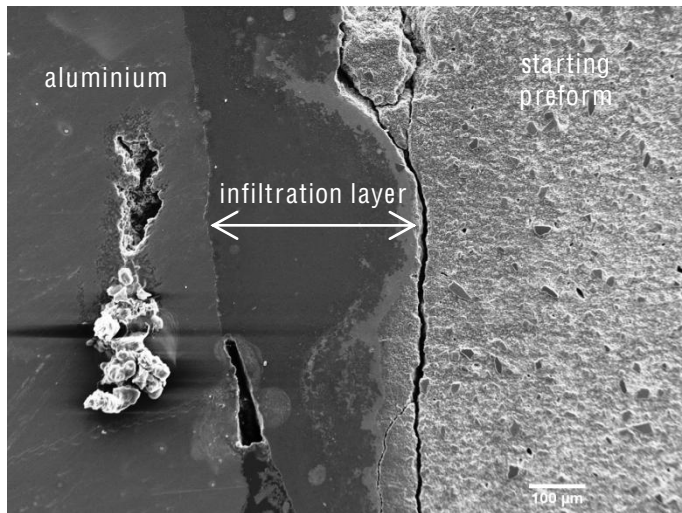


Figure 2. Low magnification secondary electron image (SEI) of sample infiltrated at 1100 °C under $pO_2 = 0.16$ atm.

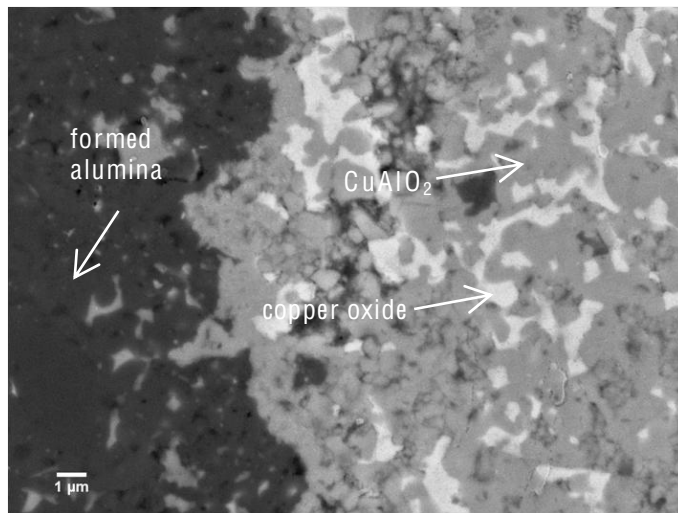


Figure 3. Backscattered electron image (BEI) of sample infiltrated at 1100 °C under $p_{O_2} = 0.16$ atm: detail of the interface between infiltration layer and starting preform.

Figure

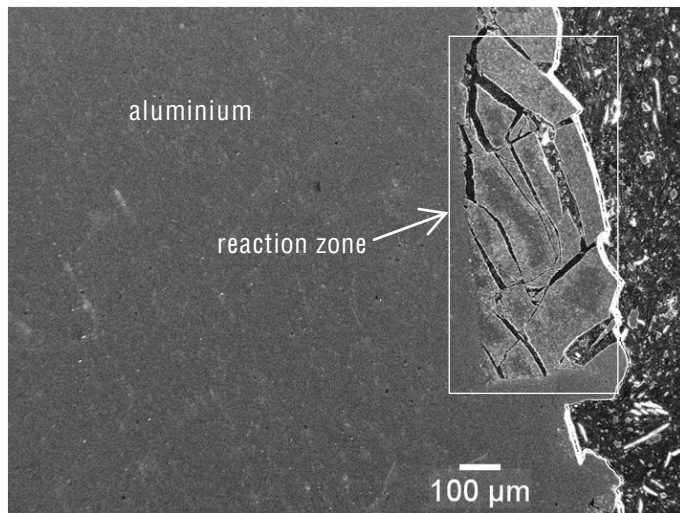


Figure 4. Low magnification SEI of sample infiltrated under $pO_2 = 8 \times 10^{-8}$ atm at 1000 °C (rectangle: incipient metal/ceramic reaction).

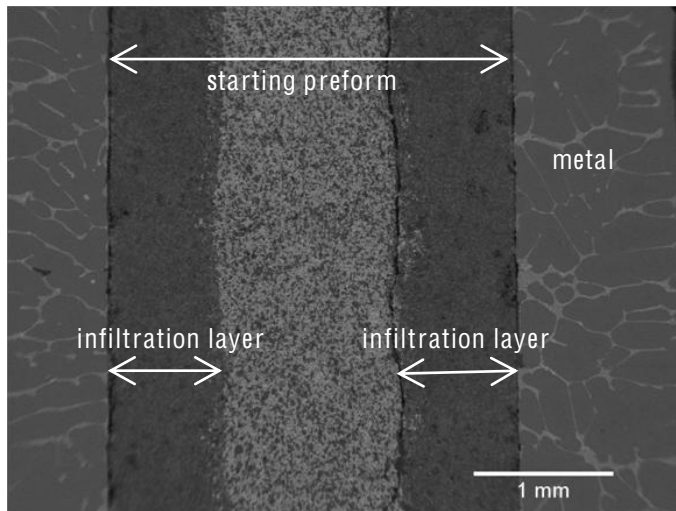


Figure 5. Low magnification BEI of infiltrated sample (1000 °C, $pO_2 = 4 \times 10^{-7}$ atm).

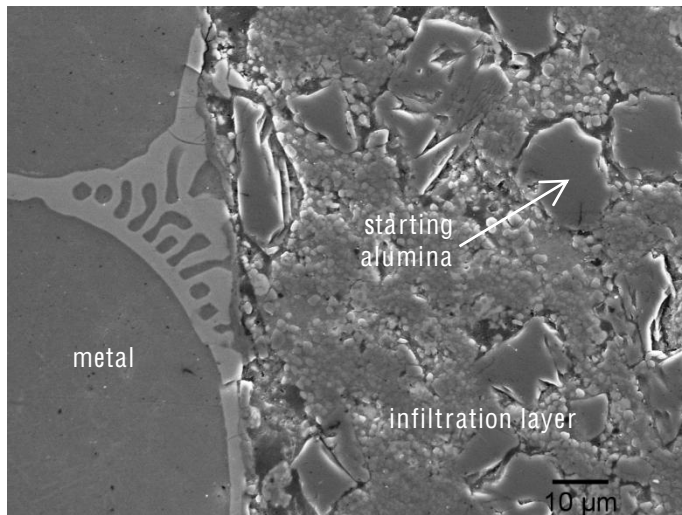


Figure 6. SEI of infiltrated sample (1000 °C, $pO_2 = 4 \times 10^{-7}$ atm): transition between metal source and infiltration layer.

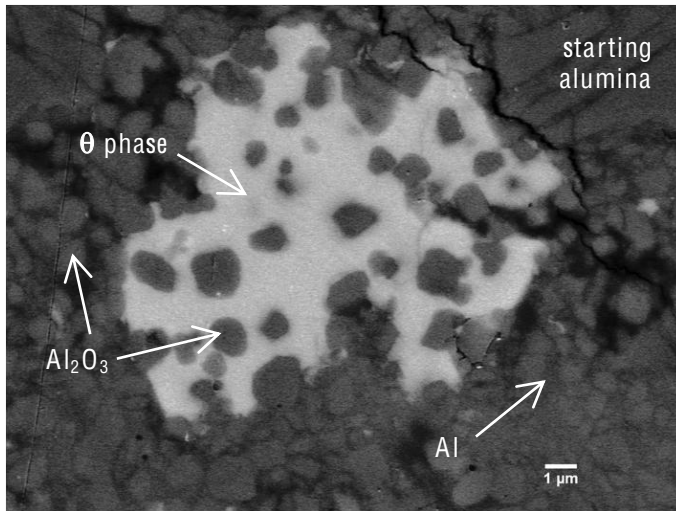


Figure 7. BEI of infiltrated sample (1000 °C, $p_{O_2} = 4 \times 10^{-7}$ atm): detail of the infiltration layer.

Figure

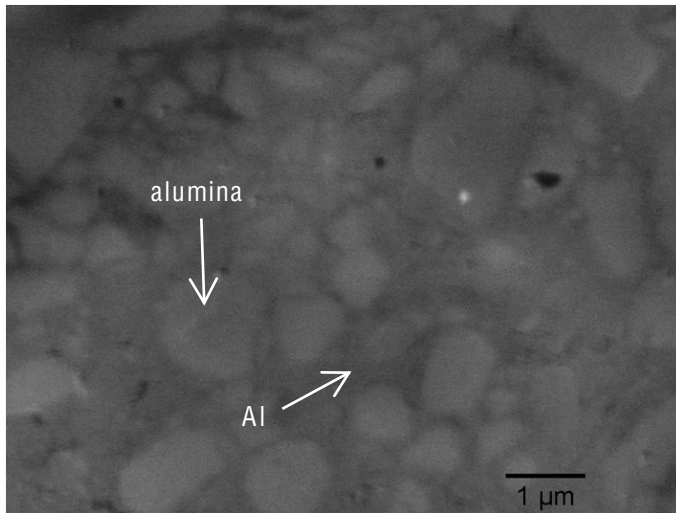


Figure 8. BEI of infiltrated sample (1000 °C, $pO_2 = 4 \times 10^{-7}$ atm): detail of formed alumina particles dispersed in Al matrix.